Electronic Supplementary Material (ESI) for Inorganic Chemistry Frontiers.

Electronic Supplementary Information for

Amino-decorated bis(pyrazolate) Metal-Organic Frameworks for carbon dioxide capture and green conversion into cyclic carbonates

Rebecca Vismara, Giulia Tuci, Nello Mosca, Konstiantyn V. Domasevitch, Corrado Di Nicola, Claudio Pettinari, Giuliano Giambastiani, Simona Galli and Andrea Rossin**

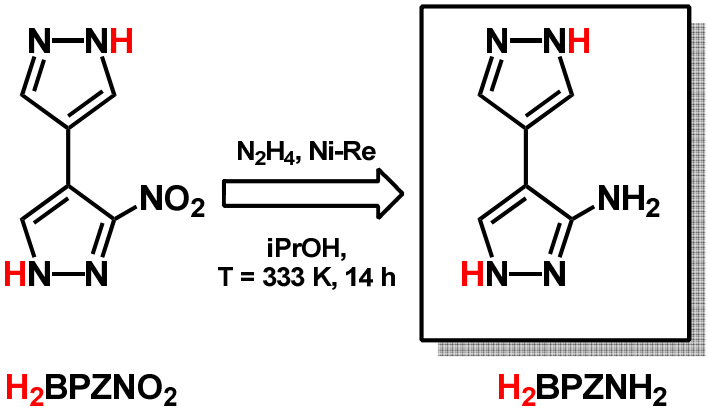

Scheme S1. Synthesis of H_2BPZNH_2.

Single-crystal X-ray Diffraction Structure Determination of H_2BPZNH_2

Diffraction data for the ligand H_2BPZNH_2 were collected at 213 K using a Stoe Image Plate Diffraction System equipped with a graphite-monochromated Mo Kα tube (λ = 0.71073 Å) and an Air Jet cooling system. φ oscillation scans (0° < φ < 185°; Δφ = 1.1°; exposure time = 14 *min* per frame) were acquired.[1] The structure was solved by direct methods and refined by full-matrix least-squares on F^2 using the programs SHELXS-97[2] and SHELXL-2014/7,[3] respectively. The structure may be solved in the monoclinic centrosymmetric space group $P2_1/c$ and refined to the final convergence values: $R1$ [$I > 2\sigma(I)$] = 0.051, w$R2$ (all data) = 0.133, GoF = 1.16 (Table S1). In this space group, the asymmetric unit contains half a bipyrazole molecule. The center of mass of the molecule resides on an inversion center and the amino group is disordered over two positions with 0.50:0.50 occupancies imposed by symmetry. Refinement of the crystal structure can be improved in the acentric space group *Pc* (Table S1), where the occupancies of the disordered amino group are refined to ~0.77:0.23 (leading to similar isotropic U values for the two components of the disorder), which differs significantly from the 0.50:0.50 in $P2_1/c$. The unequal occupancies of the two positions are clearly illustrated by a Fourier map (F_{obs}) showing the overall distribution of the electron density (Figure S1). The carbon and hydrogen atoms of the skeleton and the nitrogen atom of the disordered major component were refined anisotropically. All the hydrogen atoms were visible in Fourier maps. The bipyrazole CH- and NH-hydrogen atoms were constrained, while the amino hydrogen atoms of the disordered major component were located and included in the model

with fixed bond distances and occupancy factors of 1.0. The U_{iso} values of the hydrogen atoms were constrained at the level of 1.5×U_{eq} of the carrier nitrogen atoms or 1.2×U_{eq} of the carrier carbon atoms. Table S1 collects the main experimental details and crystallographic data. CCDC-1866302 contains the supplementary crystallographic data for H_2BPZNH_2. These data can be obtained free of charge from The Cambridge Crystallographic Data Centre *via* ccdc.cam.ac.uk/community/requestastructure.

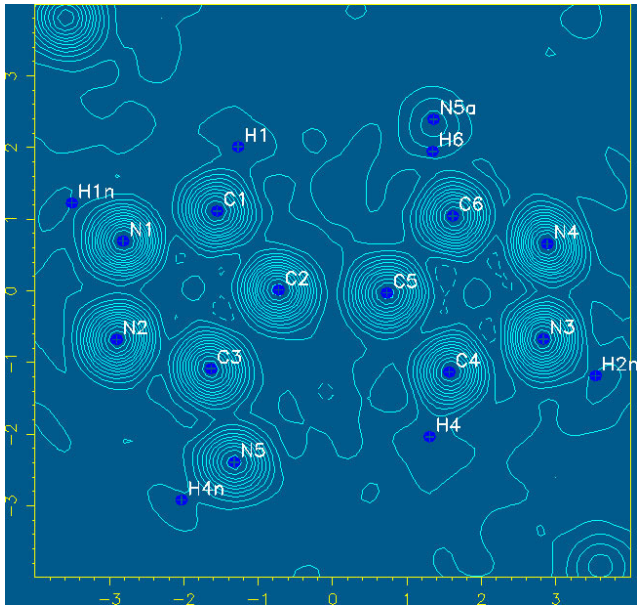

Figure S1. Slant-plane Fourier map (projection on the bipyrazole plane) showing the very unequal distribution of the electron density of the disordered amino group on the two carbon atoms (C3 and C6) of the bipyrazole backbone.

Table S1. Main crystallographic data, experimental details and structure refinement details (in *Pc* and $P2_1/c$[a]) for 3-amino-4,4′-bipyrazole.

Formula	$C_6H_7N_5$	
M [g mol^{-1}]	149.17	
T [K]	213	
Color, habit	colorless, prism	
Size [mm^3]	$0.28 \times 0.22 \times 0.22$	
Crystal system	Monoclinic	
a [Å]	8.1099(9)	
b [Å]	4.5429(4)	
c [Å]	9.3940(12)	
β [°]	107.583(13)	
V [Å^3]	329.93(7)	
μ(Mo-Kα) [mm^{-1}]	0.104	
D_{calc} [g cm^{-3}]	1.502	
Space group	*Pc*	$P2_1/c$
Z, Z'	2, 2	4, 2
$2\theta_{max}$ [°]	27.86	27.86
Measured reflns	2608	2600
Unique reflns	1416	779
Reflns with $I > 2\sigma(I)$	1029	599
Completeness [%]	99.3	99.4
R_{int}	0.0286	0.0313
Parameters refined	104	55
$R1$, w$R2$ [$I > 2\sigma(I)$]	0.0352, 0.0887	0.0512, 0.1280
$R1$, w$R2$ (all data)	0.0516, 0.0937	0.0665, 0.1316
Gof on F^2	0.916	1.162
Max, min peak [e Å^{-3}]	0.273, -0.161	0.248, -0.213

[a] In $P2_1/c$ the molecule of 3-amino-4,4′-bipyrazole resides on an inversion centre. In this case, the amino group is disordered by symmetry over two positions with occupancy 0.50:0.50. The NH_2 hydrogen atoms were located and then included with fixed bond distances and U_{iso} values constrained at the level of $1.5 \times U_{eq}$ of the carrier nitrogen atom.

Crystal and Molecular Structure of 3-Amino-4,4′-bipyrazole

H_2BPZNH_2 crystallizes in the monoclinic space group *Pc* (see above for the dichotomy *Pc vs*. $P2_1/c$). Figure S2a shows the molecular structure of the ligand with the labels adopted herein, while Figure S2b shows a portion of the crystal structure. In the latter, hydrogen bonds are present involving the pyrazole N and NH sites as complementary donors and acceptors, respectively (Table S2 and Figure S2b). These interactions yield a hydrogen-bonded 2D layer which is topologically identical to that observed for 4,4′-bipyrazole.[4] In H_2BPZNH_2, for both pyrazole rings the values of the bond angles at the nitrogen atoms [C1-N1-N2, 112.0(4)°; C3-N2-N1, 104.2(4)°; N4-N3-C4, 112.3(4)°; N3-N4-C6, 104.7(3)°] suggest that the hydrogen atoms are ordered within the NH···N network. The steric hindrance of the amino group brings about corrugation of the 2D layer, which favors the formation of weak intra-layer NH···π interactions (Table S2 and Figure S2b). These interactions clearly discriminate two different pyrazole rings: the electron-richer amino-pyrazole is more appropriate as π-acceptor. To the best of our knowledge, similar NH···π interactions, with the pyrazole ring serving as either donor or acceptor, has only few precedents in the literature.[5] A very weak inter-layer interaction involves the amino group and one NH pyrazolic site (Table S2).

Table S2. Geometry [Å, °] of the inter-molecular interactions found in the crystal structure of 3-amino-4,4′-bipyrazole.

Donor (D)	Hydrogen (H)	Acceptor (A)[a,b]	D-H	H···A	D···A	∠DH···A
N1	H1N	$N4^{i}$	0.87	2.14	2.903(4)	146
N1	H1N	$N5^{iv}$	0.87	2.58	3.198(5)	129
N3	H2N	$N2^{ii}$	0.87	2.11	2.894(4)	150
N5	H3N	Cg	0.85	2.72	3.377(4)	136
N5	H4N	$N4^{iii}$	0.89	2.50	3.165(4)	132
N1	H1N	$N5^{iv}$				

[a] Symmetry codes: (i) -1+*x*, -*y*, -0.5+*z*; (ii) 1+*x*, 1-*y*, 0.5+*z*; (iii) -1+*x*, *y*, *z*; (iv) *x*, -*y*, -0.5+*z*.
[b] Cg is defined as the centroid for the $(C1\ C2\ C3\ N1\ N2)^{ii}$ group of atoms.

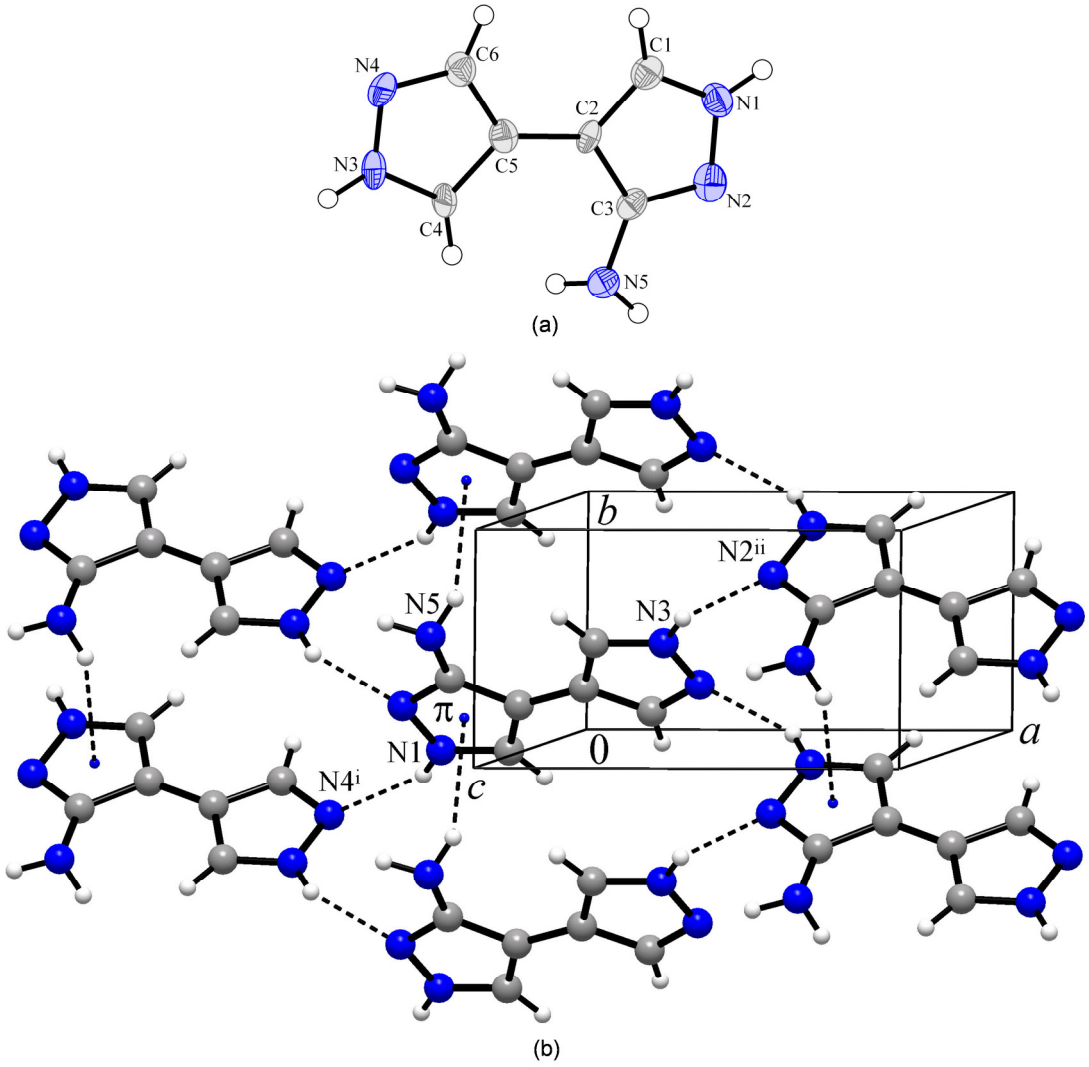

Figure S2. (a) ORTEP drawing of the 3-amino-4,4′-bipyrazole molecule at 50% probability level. Highlighted the atom labeling scheme adopted in the text. (b) Portion of the crystal structure of 3-amino-4,4′-bipyrazole viewed, in perspective, along the [001] crystallographic direction. Horizontal axis, *a*; vertical axis, *b*. The NH···N and NH···π interactions are depicted with fragmented lines. Atom color code: carbon, grey; hydrogen, light grey; nitrogen blue.

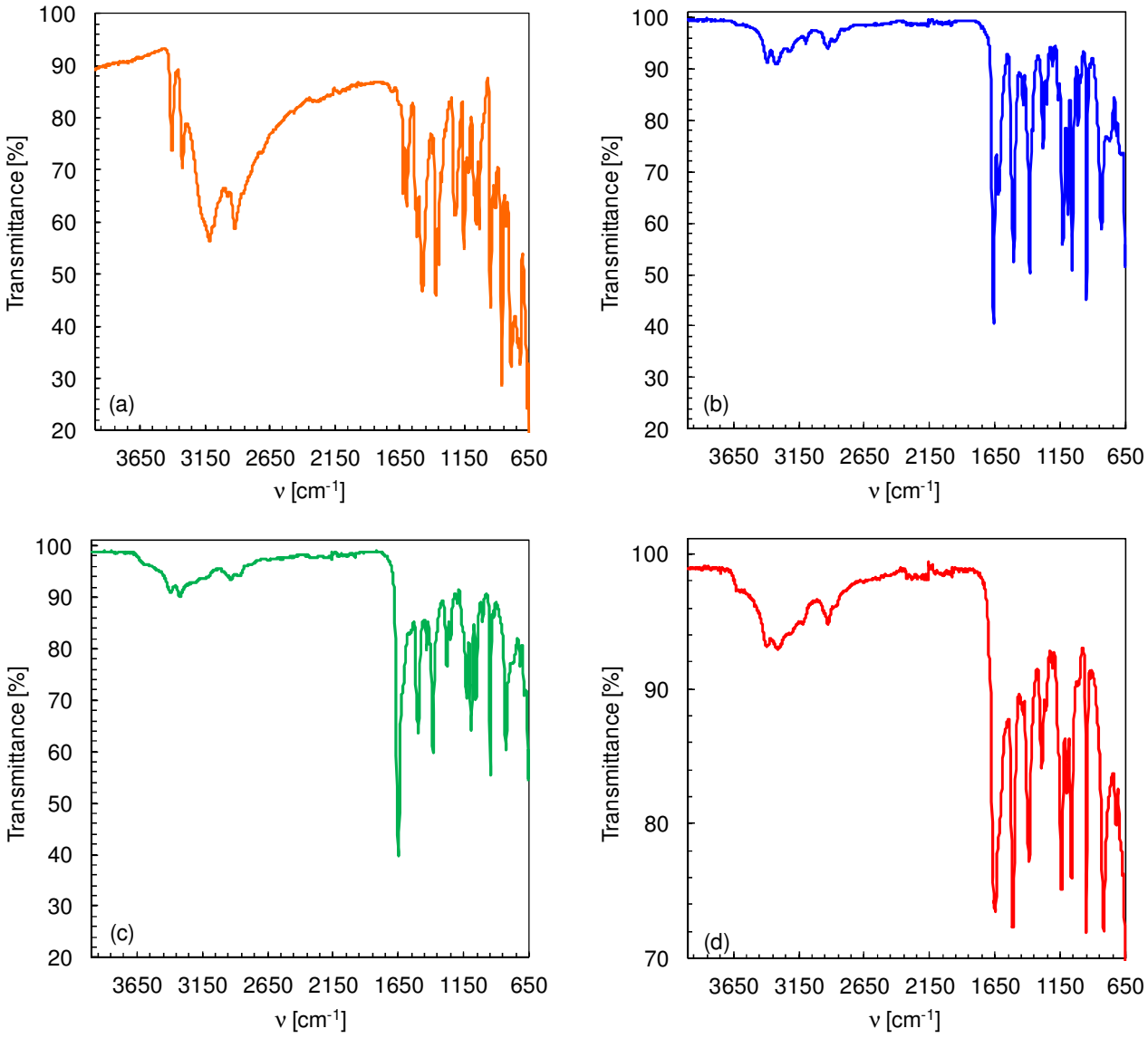

Figure S3. Infrared spectra of (a) **H_2BPZNH_2**, (b) **Zn(BPZNH_2)·DMF**, (c) **Cu(BPZNH_2)·DMF** and (d) **Ni(BPZNH_2)·DMF**.

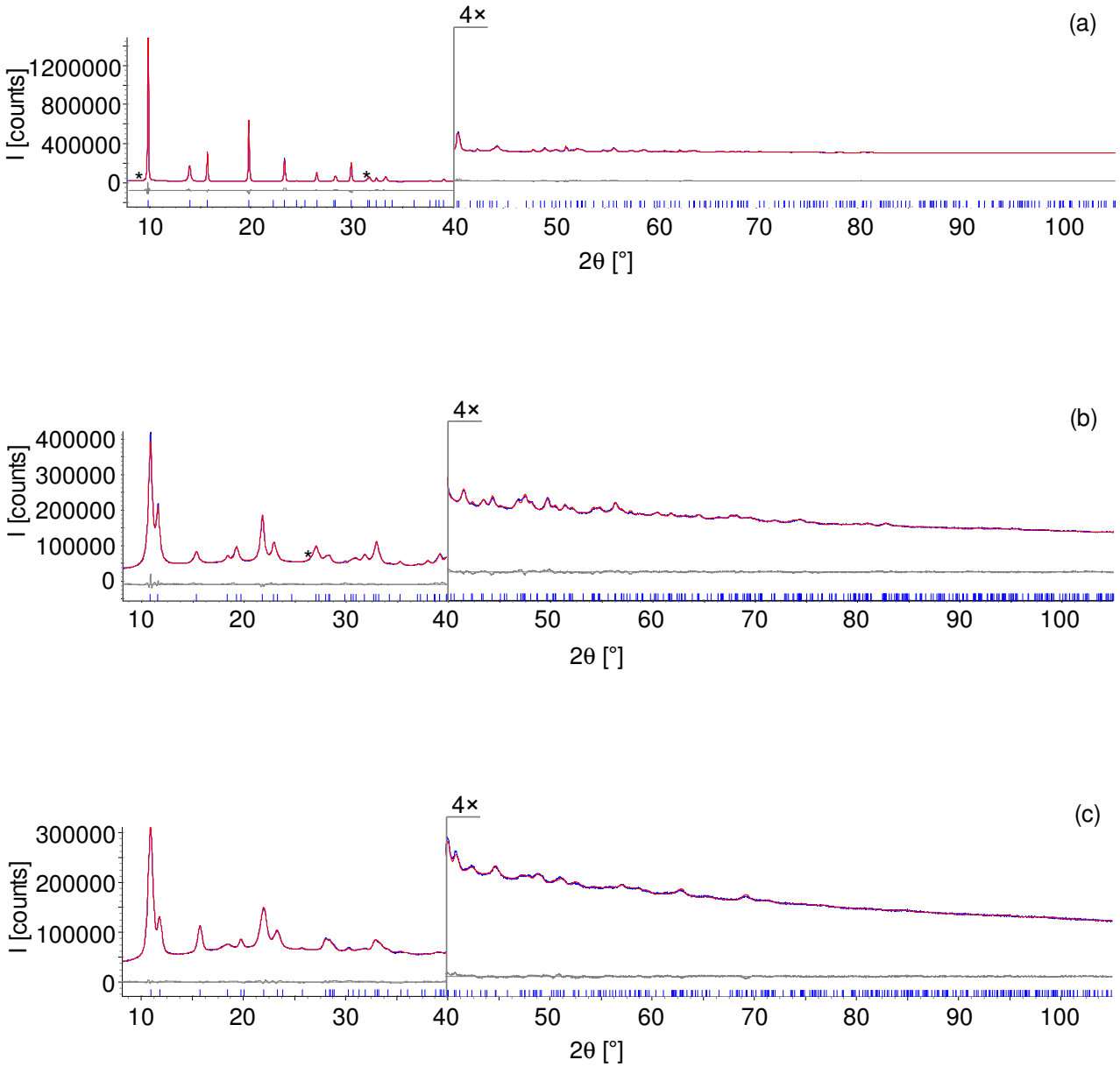

Figure S4. Graphical result of the final Rietveld refinements carried out on (from top to bottom) (a) **Zn(BPZNH$_2$)·DMF**, (b) **Cu(BPZNH$_2$)·DMF** and (c) **Ni(BPZNH$_2$)·DMF** in terms of experimental, calculated and difference traces (blue, red and grey, respectively). The blue markers at the bottom indicate the positions of the Bragg reflections. Horizontal axis, 2θ [deg]; vertical axis, intensity [counts]. The portion above ~40° has been magnified (4×). The asterisks in the pattern of **Zn(BPZNH$_2$)·DMF** and **Cu(BPZNH$_2$)·DMF** indicate peaks belonging to impurities.

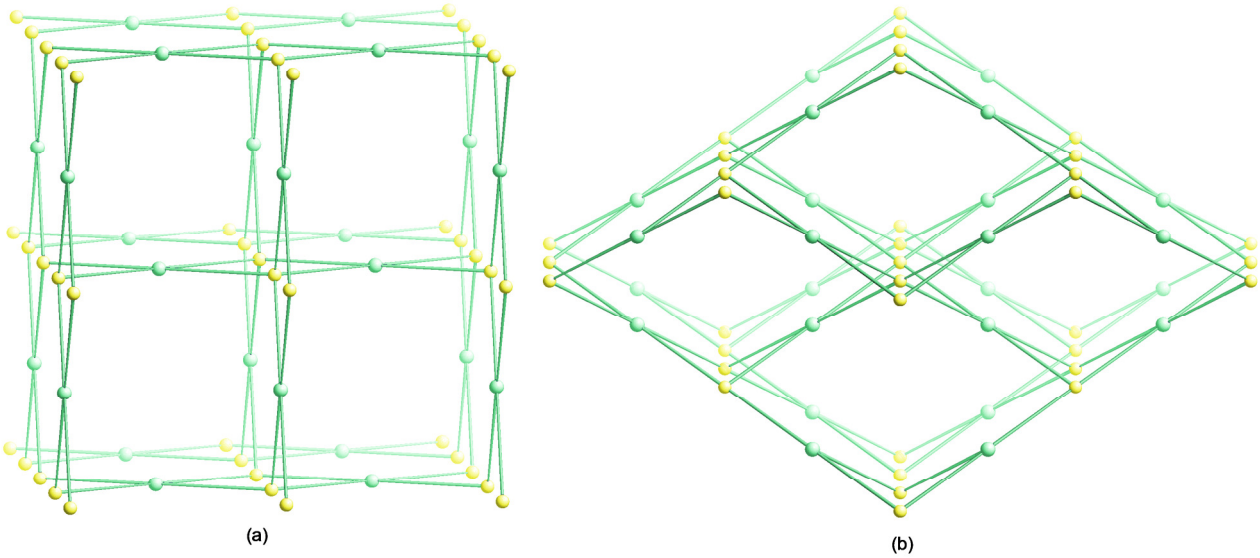

Figure S5. Schematic representation of the network topology in (a) **Zn(BPZNH$_2$)·DMF** and (b) **M(BPZNH$_2$)·DMF** (M = Ni, Cu). Both the metal ion and the ligand have been represented as tetra-connected node (yellow) and connector (light green), respectively.

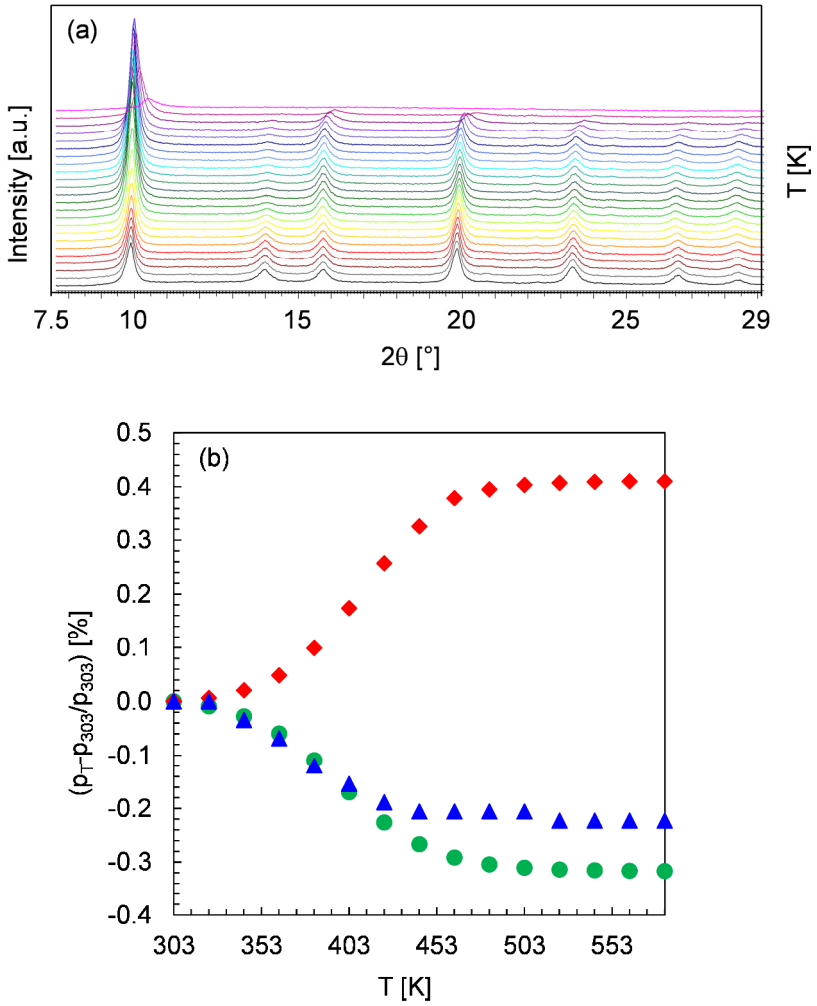

Figure S6. (a) Powder X-ray diffraction patterns of **Zn(BPZNH$_2$)·DMF** measured as a function of temperature heating in air, with steps of 20 K, in the temperature range 303 (bottom trace) – 763 (top trace) K. (b) Percentage variation of the unit cell parameters (p_T) of **Zn(BPZNH$_2$)·DMF** as a function of temperature. At each temperature, the actual values have been normalized with respect to those at 303 K (p_{30}). *a*, green circles; *c*, red diamonds; *V*, blue triangles.

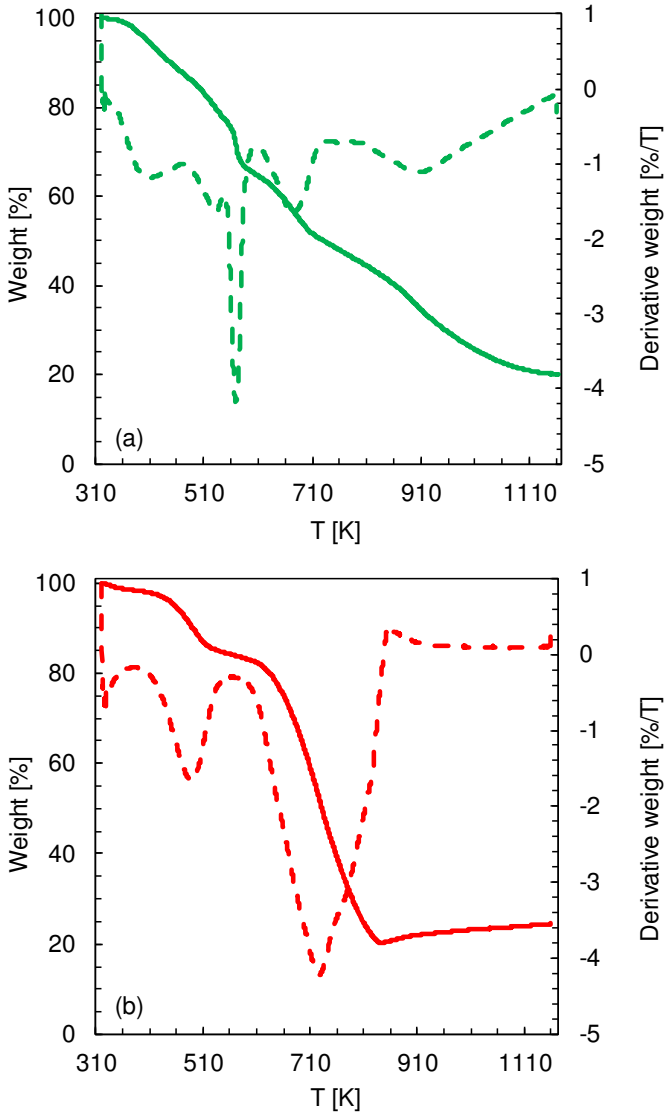

Figure S7. TGA trace (solid line) and DTG trace (dashed line) of (a) **Cu(BPZNH$_2$)·DMF** and (b) **Ni(BPZNH$_2$)·DMF**.

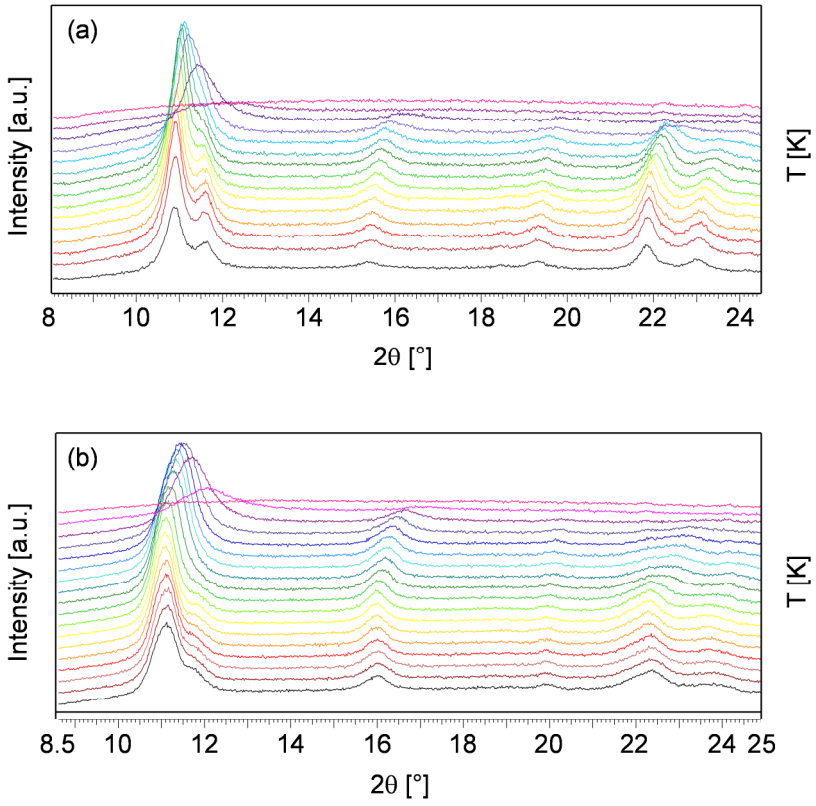

Figure S8. (a) Powder X-ray diffraction patterns measured on **Cu(BPZNH$_2$)·DMF** as a function of temperature heating in air, with steps of 20 K, in the temperature range 303 (bottom trace) – 583 (top trace) K. (b) Powder X-ray diffraction patterns measured on **Ni(BPZNH$_2$)$_2$·DMF** as a function of temperature heating in air, with steps of 20 K, in the temperature range 303 (bottom trace) – 643 (top trace) K.

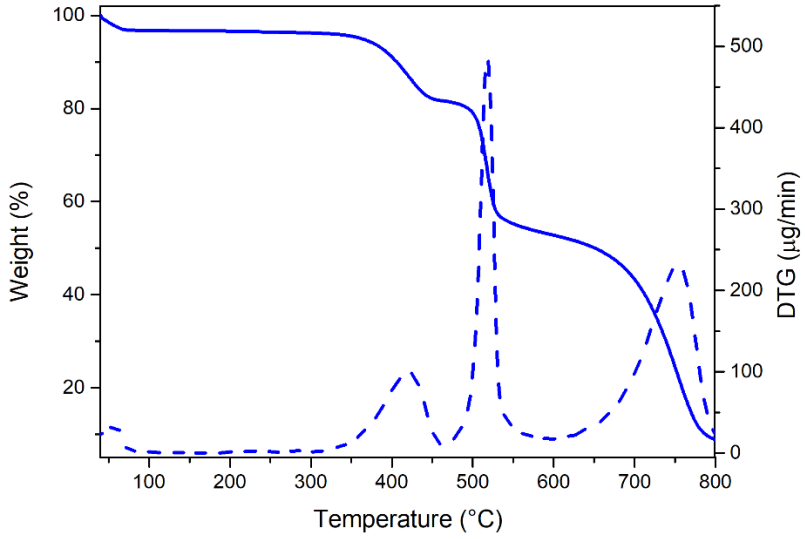

Figure S9. TGA trace (solid line) and DTG trace (dashed line) of a thermally activated sample of **Zn(BPZNH$_2$)**.

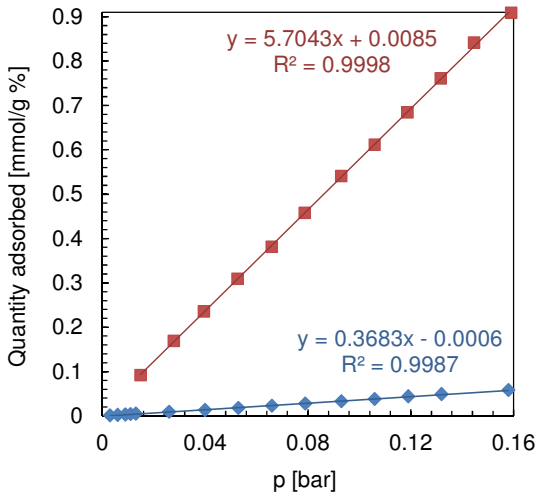

Figure S10. Comparison of the N_2 (cyan) and CO_2 (brick red) isotherms at 298 K in the 0-0.16 bar interval for the estimation of the CO_2 *vs.* N_2 selectivity of **Zn(BPZNH$_2$)** through the Henry method.

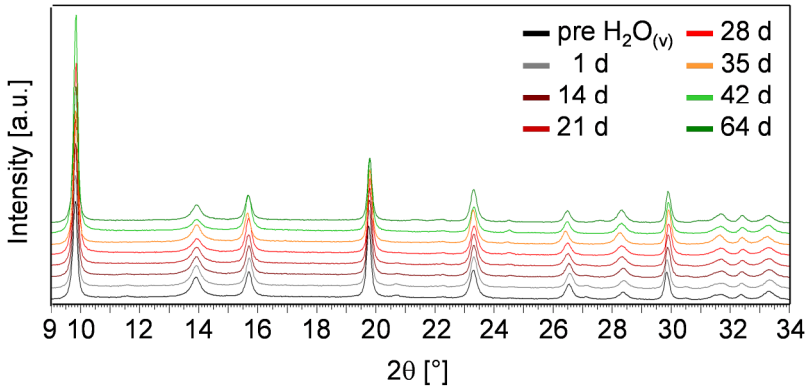

Figure S11. Powder X-ray diffraction patterns measured on **Zn(BPZNH$_2$)·DMF** before and after exposure to water vapours for certain time lapses.

Table S3. Comparison of CO_2 uptake (at 1 bar and 273 and/or 298 K) and CO_2/N_2 selectivity at 298 K among the most representative bis(pyrazolate)-containing MOFs of the *state-of-the-art*. When directly unavailable from the main article text, the values were extrapolated from the results presented (if possible).

Compound	**CO_2 uptake [mmol/g]**		**CO_2/N_2 selectivity**	**Ref.**
	273 K	298 K		
Zn-BPZNH$_2$	4.8	3.1	17 (Henry) / 14 (IAST)	This work
Zn(BPZ)	4.4	---	---	6
Zn-BPZNO$_2$	4.7	4.4	15 (Henry) / 12 (IAST)	7
Fe$_2$(BPEB)$_3$	12	9.2	25 (IAST)	8
Ni(BPEB)	8.5	5.9	19 (IAST)	8
Zn(BPEB)	8.2	5.2	21 (IAST)	8
Zn(BDP)	9.1	---	---	9
Ni(BDP)	10	---	---	9
Zn(BDP-NH$_2$)	~2.5	---	---	9
Zn(BDP-OH)	~4.5	---	---	9
Zn(BDP-NO$_2$)	~2.7	---	---	9
Co(bpdc)(BPZ)	5.5	3.1	12-28 (IAST)	10
NKU-108	4.6	2.2	27 (IAST)	11
BUT-41	4.1	2.1	14 (Henry)	12
NUS-5	---	1.8	35-46 (IAST)	13
Ni$_3$(BTPP)$_2$	---	1.7	---	14
MAF-X9	2.2	1.3	12 (Henry)	15
Co$_2$(bpdc)$_2$(H$_2$BPZ)	1.9	1.0	---	16

References

[1] Stoe & Cie. IPDS software. Stoe & Cie, 2000, Darmstadt, Germany.

[2] G. M. Sheldrick, *Acta Crystallogr.* 2008, **A64**, 112-122.

[3] G. M. Sheldrick, *Acta Crystallogr.* 2015, **C71**, 3-8.

[4] I. Boldog, E. B. Rusanov, A. N. Chernega, J. Sieler, K. V. Domasevitch, *Angew. Chem. Int. Ed.* 2001, **40**, 3435-3438.

[5] I. Boldog, E. B. Rusanov, J. Sieler, K. V. Domasevitch, *New J. Chem.* 2004, **28**, 756-759.

[6] N. Mosca, R. Vismara, J. A. Fernandes, S. Casassa, K. V. Domasevitch, E. Bailón-García, F. J. Maldonado-Hódar, C. Pettinari and S. Galli, *Cryst. Growth Des.* 2017, **17**, 3854–3867.

[7] N. Mosca, R. Vismara, J. A. Fernandes, G. Tuci, C. Di Nicola, K. V. Domasevitch, C. Giacobbe, G. Giambastiani, C. Pettinari, M. Aragones-Anglada, P. Z. Moghadam, D. Fairen-Jimenez, A. Rossin and S. Galli, *Chem.-Eur. J.* 2018, **24**, 13170-13180.

[8] S. Galli, A. Maspero, C. Giacobbe, G. Palmisano, L. Nardo, A. Comotti, I. Bassanetti, P. Sozzani and N. Masciocchi, *J. Mater. Chem. A* 2014, **2**, 12208-12221.

[9] V. Colombo, C. Montoro, A. Maspero, G. Palmisano, N. Masciocchi, S. Galli, E. Barea E. and J. A. R. Navarro, *J. Am. Chem. Soc.* 2012, **134**, 12830-12843.

[10] H. Wang, L. Jia, L. Hou, W. Shi, Z. Zhu and Y. Wang, *Inorg. Chem.* 2015, **54**, 1841-1846.

[11] Y. Jia, X. Liu, R. Feng, S. Zhang, P. Zhang, Y. He, Y. Zhang and X. Bu, *Cryst. Growth Des.* 2017, **17**, 2584–2588.

[12] Y. Zhang, T. He, X. H. Lv, B. Wang, L. Xie, X. Liu and J. Li, *J. Coord. Chem.* 2016, **69**, 3242-3249.

[13] G. Xu, Y. Peng, Z. Hu, D. Yuan, B. Donnadieu, D. Zhao and H. Cheng, *RSC Adv.* 2015, **5**, 47384-47389.

[14] A. Tabacaru, S. Galli, C. Pettinari, N. Masciocchi, T. M. McDonald and J. R. Long, *CrystEngComm.* 2015, **17**, 4992-5001.

[15] K. Chen, C. He, P. Liao, Y. Wei, P. Zhang, W. Xue, W. Zhang, J. Zhang and X. Chen, *New. J. Chem.* 2014, **38**, 2002-2007.

[16] L. Jia, Y. Zhao, L. Hou, L. Cui, H. Wang, and Y. Wang, *J. Solid State Chem.* 2014, **210**, 251-255.